

Digital logarithmic airborne gamma ray spectrometer^{*}

ZENG Guo-Qiang(曾国强)¹⁾ ZHANG Qing-Xian(张庆贤) LI Chen(李晨) TAN Cheng-Jun(谭承君)
 GE Liang-Quan(葛良全) GU Yi(谷懿) CHENG Feng(程锋)

Chengdu University of Technology, Chengdu 610051, China

Abstract: A new digital logarithmic airborne gamma ray spectrometer is designed in this study. The spectrometer adopts a high-speed and high-accuracy logarithmic amplifier (LOG114) to amplify the pulse signal logarithmically and to improve the utilization of the ADC dynamic range because the low-energy pulse signal has a larger gain than the high-energy pulse signal. After energy calibration, the spectrometer can clearly distinguish photopeaks at 239, 352, 583 and 609 keV in the low-energy spectral sections. The photopeak energy resolution of ¹³⁷Cs improves to 6.75% from the original 7.8%. Furthermore, the energy resolution of three photopeaks, namely, K, U, and Th, is maintained, and the overall stability of the energy spectrum is increased through potassium peak spectrum stabilization. Thus, it is possible to effectively measure energy from 20 keV to 10 MeV.

Key words: logarithmic amplifier, airborne gamma ray spectrometer, energy calibration, wide-range spectrum measurement, cosmic rays measurement

PACS: 29.30.kv **DOI:** 10.1088/1674-1137/38/7/076001

1 Introduction

Airborne gamma ray spectrometry is a radiometric method. A gamma ray spectrometer system is installed on an aircraft to measure the gamma ray spectra of surface rocks and ore, from which the total radioactivity (or the intensity of radioactivity) and the contents of potassium, uranium and thorium are determined [1, 2]. The airborne gamma ray spectrometry method is also highly appropriate for large scale environmental surveys of areas of potentially contaminated ground, as well as for studies of the environment of nuclear sites for reference purposes [3].

Gamma-ray spectrometer (GRS) has been proven to be a powerful instrument for remote measuring the abundance of chemical elements, such as C, O, Mg, Al, Si, K, Ca, Fe, Th, and U, on the planetary surface. The GRS onboard Chang'E-1 satellite (a lunar polar orbiter at the altitude 200 km and in operation for one year) was conceived to map the lunar surface in the first Chinese lunar mission in 2007. The detector of GRS can detect the gamma rays of the moon at energies between 300 keV–10 MeV. In this wide range spectrum measurement, the energy interval of x -axis is 22.14 keV. Another reason why the energy resolution at 662 keV is 8.3% is because the peak at 583 keV and 727 keV from Th lines overlapped with the peak at 609 keV from element U [4].

In the above situation, the gamma ray energy in gamma ray spectrometry ranges up to 10 MeV. The analog to digital converter (ADC) resolution and input signal range in the system are determined. Then, the pulse signals of the low-energy spectral section are significantly condensed under a linear amplifier to ensure that the pulse signals of the maximum energy 10 MeV can be measured and analyzed. The low-energy spectral section among the collected spectrum is also condensed and the photopeak energy resolution of the section significantly become worse; therefore, it is hard to satisfy the airborne gamma ray spectrometry survey [5, 6].

Segmented measuring is a possible solution that may be applied to guarantee the photopeak energy resolution of both high-energy and low-energy spectra simultaneously. In other words, it should use two spectrometers that have different amplifier gains to measure the high and low energy spectra individually. This method requires separate energy calibration and merges the two spectra together, which increases the hardware expense and data processing difficulty. Effective spectrum stabilization in the airborne gamma ray spectrometer measurement applies the natural potassium (K) photopeak as the characteristic photopeak. The segmented measuring method mentioned above could only stabilize the high energy spectra by natural potassium photopeak, but failed at the low energy spectra because the K photopeak

Received 30 July 2013

^{*} Supported by National Natural Science Foundation of China (40904054) and National High Technology Research and Development Program 863 (2012AA061803)

1) E-mail: zgq@cdut.edu.cn

©2014 Chinese Physical Society and the Institute of High Energy Physics of the Chinese Academy of Sciences and the Institute of Modern Physics of the Chinese Academy of Sciences and IOP Publishing Ltd

has been truncated in the low energy spectrometer. Large spectrum drift of the multi-crystal airborne gamma ray spectrometer measurement occurs, which significantly decreases the energy resolution of the photopeak of the multi-crystal merged spectrum [7].

The effective number of bits (ENOB) of ADC in the digital spectrometer decreases with the increase of the conversion rate and the input signal ranges of the digital spectrometer. The lower ENOB has lower resolution to pulse signals of the low energy gamma ray [8, 9]. For example, an ADC full scale input voltage range of 4 V, which corresponds to the pulse signal amplitude of the 10 MeV gamma ray, leads to pulse signal amplitude of only 8 mV, which corresponds to a 20 keV gamma ray, and is almost drowned out by the background noise. If a linear amplifier has to be used then the low-energy spectra are compressed and they cannot be clearly shown, hence its signal dynamic range should be narrow. Using a logarithmic amplifier, the pulse signals from the low-energy radionuclides are greatly amplified, whereas the pulse signals from the high-energy radionuclides are less amplified. The photopeak interval of the high-energy rays among the produced logarithmic spectrum is consequently condensed and reduces the abundant blank spaces, whereas the photopeak interval of low-energy rays is widened. The result from the low-energy nuclides avoids wasting the blank spaces in the high-energy spectrum and significantly widens the low-energy spectrum. It also recovers the energy resolution of the low-energy photopeak by maintaining the same energy resolution of the high-energy photopeak. This result takes full advantage of the channel address and resolution of the ADC.

Therefore, the logarithmic amplifying circuit is introduced in this paper to conduct the logarithmic calculation to the pulse signals. In doing so, this paper aims to condense the high-energy spectrum, widen the low-energy spectrum, and guarantee the energy resolution of both the high-energy and low-energy spectra.

2 System framework

The components of the digital logarithmic airborne gamma ray spectrometer are shown in Fig. 1. The Ping-Pong buffer FIFO (First In First Out) memory coordinated with the quick interrupter built inside the ARM chip to achieve real-time parallel spectrum transmission and spectrum acquisition. The magnetic coupling serial port isolated the communication circuit through the ADM3251E and electrically isolated the digital spectrometer from the outside environment and serial port data communication. The maximum data transmission rate of the chip was 460 kbps. It had an inbuilt DC-DC isolated power supply, which simplified the circuit design.

2.1 Design of digital pulse height analyzer

Since the entering pulse signal is transformed through the logarithmic amplifier (instead of the usual fast-rising, slow decline of the double exponential signal), we cannot use a digital trapezoidal shaper to analyze pulse height [10]. In this paper, the state machine based sampling method is used to achieve the maximum number pulse amplitude extraction, which is described as follows:

Construction of a width of 16 digital moving average window: average value of the first eight numbers defined as “avg_forw”, average of the last eight numbers defined as “avg_back”, “ThUp” defined as a variable indicates upper threshold of comparator, “ThDn” defined as a variable indicates lower threshold of comparator, “base” defines as a variable indicates baseline value, “height” defines as a variable indicates pulse amplitude.

State1: when expression (1) is true it initializes variable “min” and jumps to state2;

$$\text{avg_back} < \text{avg_forw}. \quad (1)$$

State2: read cycle variable of “avg_forw”, and put the minimum value into “min”; when expression (2) is

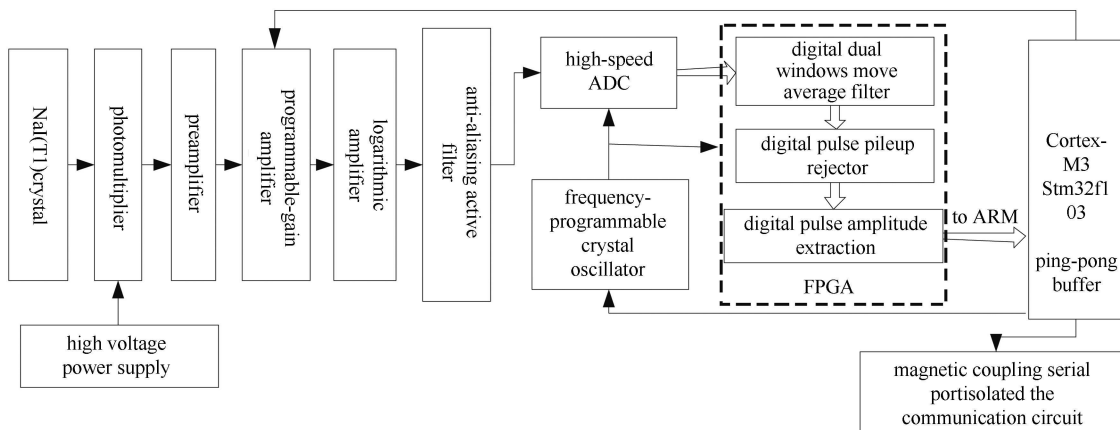


Fig. 1. System framework of the digital logarithmic airborne gamma ray spectrometer.

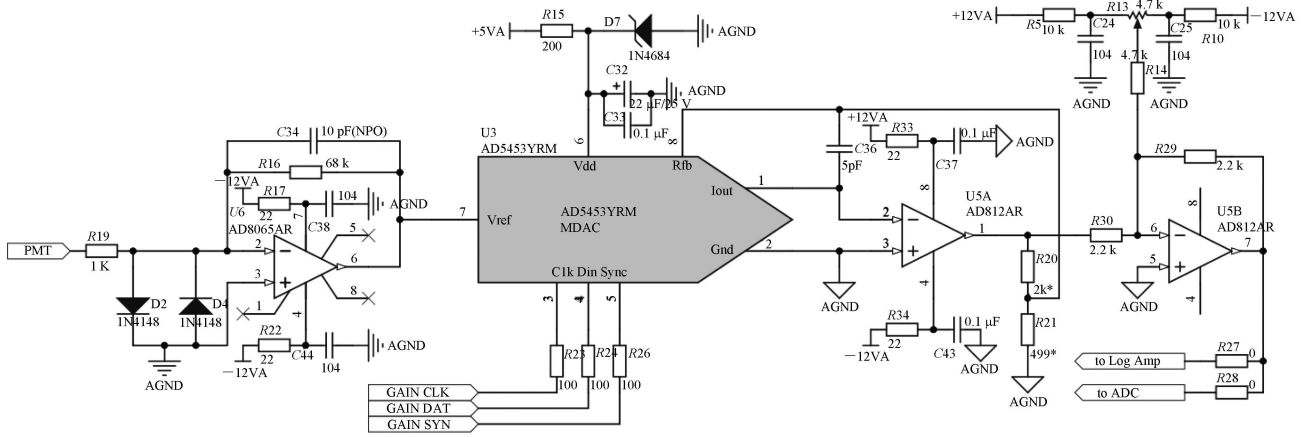


Fig. 2. Schematics of preamplifier and programmable gain amplifier.

true, assigns variable “min” to variable “base”, and initializes variable “max”, and jumps to state3;

$$\text{avg_forw} > \text{avg_back} + \text{ThUp}. \quad (2)$$

State3: read cycle variable of “avg_forw”, and put the maximum value into “max”; when expression (3) is true, assigns variable “height” with result of “max” minus “base”, thereafter the output current variable “height” to ARM controller; jumps to state1;

$$\text{avg_forw} \leq \text{avg_back} + \text{ThDn}. \quad (3)$$

The foregoing method can signal filtering noise reduction, automatic tracking baseline, it can also distinguish two overlapped pulse signals. ADC sampling rate is higher, the ability of the pile-up correction will also be more powerful [11]. In a practical application of the ADC the sampling rate should be adjusted to the width of the moving average window in order to obtain the best filtering effect. By adjusting ThUp with ThDn, the value can filter out interfering signals in order to guarantee that only the correct signal is processed by amplitude extraction.

This method does not do an exact dead time correction. Taking into account the ADC sampling rate of 40 MHz, the moving average window is 8 points, the signal rise time is 400 ns, and the system dead time is approximately 500 ns. Hence, we compensate for dead time loss after each measurement according to the measuring time and total number of pulse signals [12].

2.2 Design of the preamplifier and programmable gain amplifier

Figure 2 shows the preamplifier and programmable gain amplifier designed in this system. A low bias current of high speed voltage amplifiers AD8065AR was selected to serve as the preamplifier. The AD8065AR, configured for inverting amplifier mode, converted the current signal output from PMT to voltage signal. D_1 , D_2 limited

the voltage to not exceed ± 0.6 V of inverting input of U_6 , and protected the input of U_6 in order to not be damaged by a surge voltage. The programmable gain amplifier was designed by using a high speed multiplying DAC (AD5453YM [13]) that has a 14 bit resolution. This DAC with 10 MHz multiplying bandwidth could meet the requirements of this system. The power supply of an AD5453YRM is 3.3 V, with STM32 control signal output level matching, and its Vref is connected with preamplifier output, Vref input impedance is approximately 10 k Ω , which can withstand a ± 12 V maximum input signal. The input voltage signal is converted to a current signal and then it converted the current signal to voltage signal through the high-speed current op amp AD812AR. Fig. 2 shows that the amplifier works on a logarithmic amplification mode when soldered R_{27} , removed R_{28} , signal of U_{5B} through the logarithmic amplifier stage and input to ADC; when removed R_{27} , soldered R_{28} , signal of U_{5B} direct output to the ADC, and so works in a linear amplification mode. After this preamplifier, the output pulse signal has a peaking time [14] of 400 ns and a falling time of 600 ns.

Compared with the conventional digital airborne gamma ray spectrometer [15], the new digital logarithmic airborne gamma ray spectrometer adds a new logarithmic amplifier behind the preamplifier to logarithmically convert the pulse signals.

3 Design of logarithmic amplifier

The logarithmic amplifier designed in this paper is directly applied to amplify the pulse signal from the preamplifier, which has not been shaped, which is unlike that in Ref. [16]. The accuracy of the analyzer when a pulse pile-up happens will deteriorate the slow rising time of the pulse signal. Hence, the important difference of this logarithmic amplifier is fast enough to preserve the short rising time of a pulse signal from the amplifier. The

actual logarithmic amplifier is generally equipped with both linearity and logarithmic amplification, which is a linear amplifier with a larger gain for a weak input signal. However, the linear amplifier can become a logarithmic amplifier for strong input signals and its gain will decrease with increasing input signal amplitude. Common types of logarithmic amplifiers include: basic logarithmic amplifier, baseband logarithmic amplifier, and demodulating logarithmic amplifier.

The logarithmic amplifier used for precise pulse amplitude sampling has to have excellent DC precision and frequency response, which cannot be satisfied by common basic logarithmic amplifiers because the pulse signals are double exponential signals that rise quickly but decay slowly. LOG114, a true logarithmic amplifier made by TI Company, which has high DC precision, high speed, and high accuracy [17]. The bandwidth for small signals is larger than 10 MHz, which meets the requirements of this research when I_{ref} is at 10 μ A. Fig. 3 shows the internal functional framework of LOG114, which reveals that LOG114 logarithmically transforms the current inputs I_1 and I_2 into V_{BE} voltage of the PN junction of the internal Q_1 and Q_2 . Q_1 and Q_2 can overcome the DC error caused by the temperature drift because of the similar manufacturing technique and excellent matching of the audion. The V_{BE} voltage output by Q_1 and Q_2 is differently amplified by the A_3 installed inside the LOG114, which further overcomes the DC error caused by the temperature drift. In addition, A_4 and A_5 can amplify the signal output of A_3 . A 2.5 V output reference source exists inside LOG114, which can be connected to Pin3 through the resistance to produce the reference current I_2 .

Based on the LOG114 datasheet [18], the output voltage of the operational amplifier A_3 is

$$V_{LOGOUT} = 0.375 \times \lg(I_1/I_2) + V_{CMIN}. \quad (4)$$

The DC offset can be adjusted by altering V_{CMIN} . Given the bandwidth characteristics of the operational amplifiers A_4 and A_5 in LOG114, and the unsatisfying input offset voltage, this research applies the externally connected AD8065, which is a high-speed but low-noise operational amplifier, for signal amplification. The temperature coefficient of the internal reference source of LOG114 [16] is ± 25 ppm/ $^{\circ}$ C. REF192ES is applied as the reference source because the temperature characteristic of the system worsens when the I_2 reference current produced by the internal reference source of LOG114 is used. The temperature coefficient of REF192ES [19] is 2 ppm/ $^{\circ}$ C and its output voltage is 2.5 V, which can increase the temperature stability of I_2 . The practical design is shown in Fig. 4.

The pulse signals output by the preamplifier are voltage signals that have to be converted into current signals (I_1) when output to the logarithmic amplifier. A larger I_1 leads to a wider signal bandwidth based on the datasheet of LOG114. Therefore, I_1 is expected to be as large as possible. However, the fitting degree of the output logarithm decreases when $I_1 > 2$ mA; thus, this study determines $I_{1MAX} = 2$ mA. The amplitude of pulse signal output by the preamplifier corresponding to the 10 MeV gamma ray is assumed to be 10 V; then, $R_7 = 10 \text{ V} / 2 \text{ mA} = 5 \text{ k}\Omega$. The DC level of the V_{in} signal is 0 V and the corresponding I_1 value is 0 mA when the pulse signal is absent. Eq. (4) states that the DC level

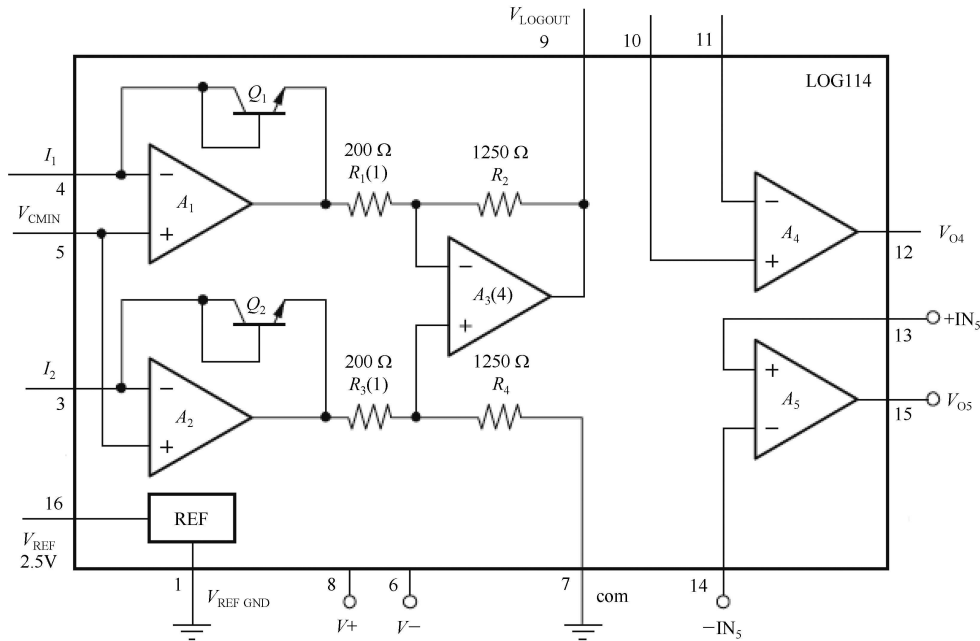


Fig. 3. Internal functional framework of LOG114.

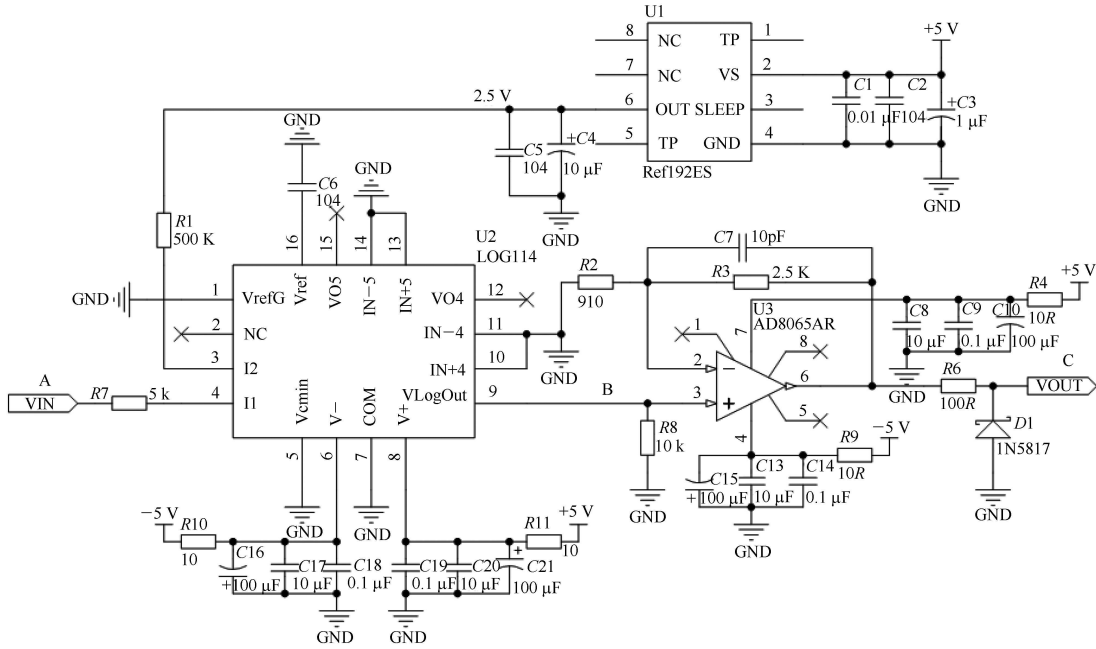


Fig. 4. The circuit of the high-speed and high-accuracy logarithmic amplifier by LOG114.

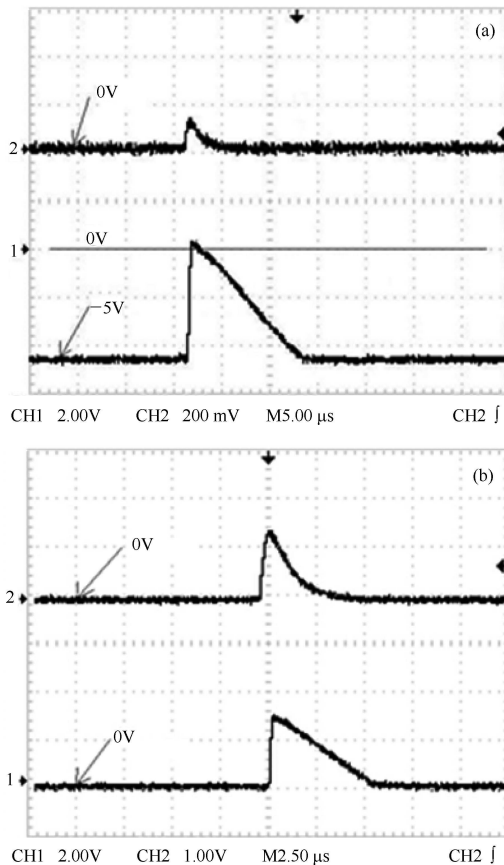


Fig. 5. (color online) Signal of channel 2 in Fig. (a) and Fig. (b) comes from linear preamplifier's output; Signal of channel 1 in Fig. (a) comes from point B of Fig. 4; Signal of channel 1 in Fig. (b) comes from point C of Fig. 4.

of the output signal of LOG114 has a negative power supply (-5 V). The DC level would be logarithmically amplified by LOG114 once pulse signals are present, and the output pulse would be at the B point in the circuit of Fig. 4 (Fig. 5(a)). The positive amplitude part of the pulse signal in Fig. 5(a) is apparently the actual amplitude of the input pulse signal after the logarithmic calculation. Therefore, it is necessary to apply direct coupling for the connection of the output signals of LOG114 and next-stage circuit AD8065. The D_1 amplitude limiter on the post-amplifier output cuts the negative part of the outputting signal by using R_6 (Fig. 4). A comparison between the original pulse signal and the quasi-triangular signal is shown in Fig. 5(b). The quasi-triangular signal is the output of the pulse signal, which is logarithmically amplified and shaped, and whose amplitude is limited by the operational amplifier, as shown in point C in the circuit of Fig. 4. The output baseline is fixed at 0 V after the amplitude is limited by R_6, D_1 .

4 Relationship between reference current and spectrum

Equation (4) of the logarithmic amplifier output states that the output of the pulse signal through the logarithmic amplifier is related to the reference current I_2 . The V_{CMIN} that is used to adjust the DC offset will be connected to the ground to maintain a simple subsequent design when the new DC offset is introduced. The new DC offset only has $\log_{10}(I_1/I_2) > 0$ to ensure the output of the logarithmic amplifier $V_{\text{LOGOUT}} > 0$;

that is, $I_1 > I_2$. Therefore, I_2 is used to set the minimum energy of the pulse signal. A larger I_2 or I_1 leads to a wider bandwidth of the DC signal of LOG114, a better high-frequency response, and a smaller pulse distortion based on the datasheet of LOG114. However, a larger I_2 would surely increase the lower energy threshold of the pulse signal, which necessitates the setting of an appropriate I_2 . Only the value of I_2 is changed to obtain the optimal I_2 . The spectra under the different I_2 are measured for comparison. Fig. 6 shows that, when I_2 is valued too high, the low-energy part of the spectrum is cut. The low-energy part can also be completely measured when I_2 is valued at $5 \mu\text{A}$. Therefore, when $I_2=5 \mu\text{A}$ and $R_1=2.5 \text{ V}/5 \mu\text{A}=500 \text{ k}\Omega$, the small signal bandwidth of A_1 is about 10 MHz.

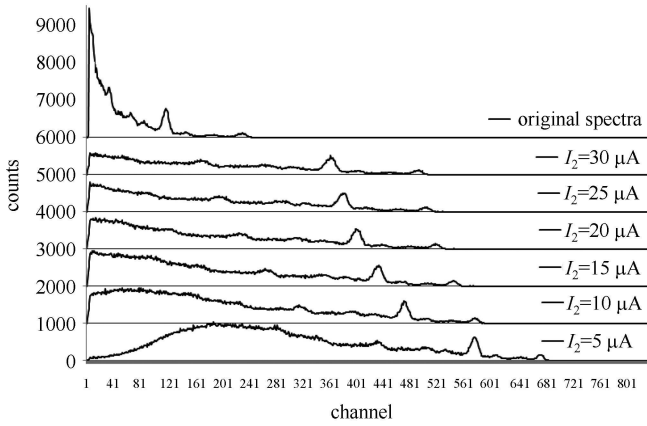


Fig. 6. Natural gamma ray spectra measured with different reference currents.

The output of logarithmic amplifier ($V_{\text{LOGOUT}} = \lg(I_1/I_2)$) is inversely proportional to the I_2 current. Hence, a smaller I_2 current will enable a wider natural gamma ray spectrum.

5 Energy calibration of logarithmic spectrum

Energy calibration is essential before calculating the peak area and the content of the obtained logarithmic spectrum [20, 21]. The energy characteristic of the obtained spectrum is logarithmic because the pulse signals are processed with logarithmic transformation. Next, we will discuss the energy calibration of the spectrum that takes a logarithmic characteristic since its horizontal axis is necessary. The maximum voltage for the preamplifier to the output pulse signal is assumed as V and the photon energy is E . Given that the preamplifier is a linear system, where a and b are constants, V can be determined as

$$V = a \times E + b. \quad (5)$$

The reference voltage of ADC is V_{REF} , the post amplification of logarithmic amplifier is G , and the corresponding channel address after the ADC conversion is ch when the output pulse signals of the preamplifier enter the ADC after being logarithmically amplified by the logarithmic amplifier and if the resolution of the ADC is 2^n . This result can be expressed as

$$\frac{G \times \lg(V/R/I_2) \times 2^n}{V_{\text{REF}}} = ch. \quad (6)$$

Where R is the input resistance to convert the input voltage signals into current signals and I_2 is the reference current of LOG114, both of which are constants. Therefore, $I_2/R = K$. Eq. (6) can be transformed as

$$\lg\left(\frac{V}{K}\right) = \frac{V_{\text{REF}} \times ch}{G \times 2^n}, \quad (7)$$

Then,

$$V = K \times e^{\frac{V_{\text{REF}} \times ch}{G \times 2^n}}. \quad (8)$$

Equation (5) is substituted into Eq. (7). Then,

$$a \times E + b = K \times e^{\frac{V_{\text{REF}} \times ch}{G \times 2^n}}. \quad (9)$$

Finally,

$$e = \frac{K}{a} e^{\frac{V_{\text{REF}} \times ch}{G \times 2^n}} - \frac{b}{a}. \quad (10)$$

Equation (10) reveals that an exponential functional relationship exists between the channel address and the ray energy. Therefore, the equation can be set as follows:

$$A_1 = K/a, \quad (11)$$

$$A_2 = G \times 2^n / V_{\text{REF}}, \quad (12)$$

$$A_3 = -b/a. \quad (13)$$

Equations (11), (12), and (13) are substituted into Eq. (10). Then,

$$e = A_1 \times e^{ch/A_2} + A_3. \quad (14)$$

A_1 , A_2 , and A_3 can be obtained through the exponential functional curve fitting on the energy of several groups of characteristic peaks and channel addresses. The substitution accomplishes the energy calibration of the logarithmic spectrum. Fig. 7 shows the practical measured energy calibration curve, which has a reference current of $5 \mu\text{A}$. The calibration source of ^{241}Am , ^{212}Pb , ^{220}Pb , ^{214}Bi , ^{226}Ra , ^{238}Th , ^{137}Cs , ^{40}K and ^{208}Tl are selected.

The energy calibration is calculated using Origin software (Fig. 8), which obtains both the calculation fitting degree of 0.999925 and the calculation result.

$$E = 14.561487 \times e^{0.006522ch}. \quad (15)$$

The spectrum after the energy calibration based on the calculation result of Eq. (15) is shown in Fig. 7(b), which shows that the photopeaks at 239, 352, 583, and

609 keV in the low-energy section can be obviously distinguished. Furthermore, the photopeak width of K, U, and Th are determined based on the energy interval selection approach of the airborne gamma ray spectrometry survey conducted by the International Atomic Energy Agency (IAEA) [21], as shown in Table 1.

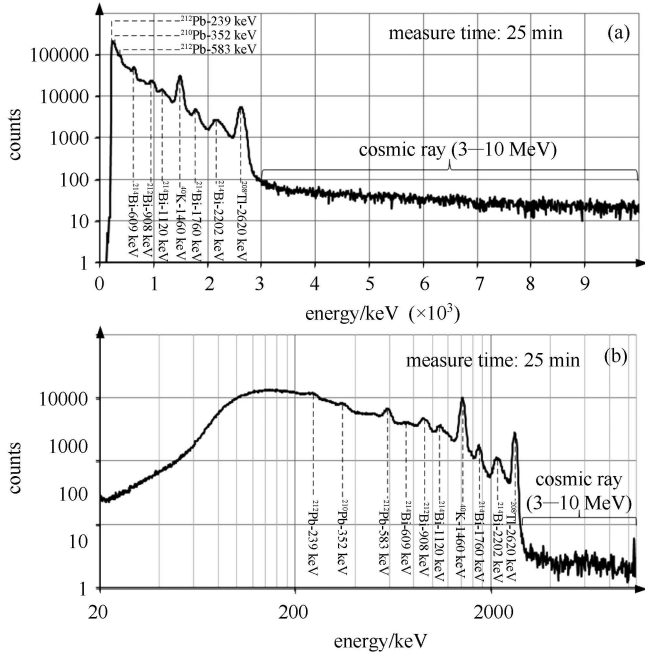


Fig. 7. Contrast of natural gamma ray spectra with energy range of 20 keV–10 MeV measured in the same conditions; (a) Natural gamma ray spectrum measured in linear mode; (b) natural gamma ray spectrum measured in logarithmic mode.

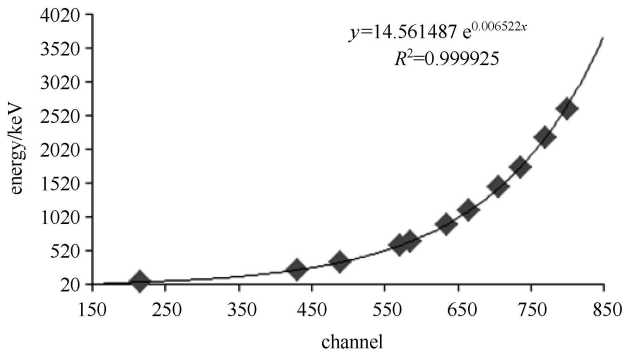


Fig. 8. Energy Calibration Curve.

The energy interval division approach established by IAEA is also applicable on the logarithmic spectrometer, which achieves no overlapped energy intervals in the characteristic spectrum with all photopeaks independent from each other. Therefore, the application of the logarithmic calculation does not affect the high-energy

gamma ray spectrum but widens the low-energy gamma ray spectrum, which is beneficial for the utilization and observation of the low-energy gamma ray spectrum and increases the utilization rate of the spectral data.

Figure 7(a, b) shows the natural gamma ray spectra with energy range of 20 keV–10 MeV when measured with a digital airborne gamma ray spectrometer working in linear and logarithmic modes, respectively. The measurement is carried out by using 4inch*4inch*16inch NaI(Tl) crystals of ¹³⁷Cs intrinsic energy resolution of 7.8%, which are produced by Saint-Gobain Inc.

Table 1. Recommended windows for natural radioelement mapping (IAEA, 1991).

window name	isotope used	gamma-ray energy/keV	energy window/keV
potassium	⁴⁰ K	1460	1370–1570
bismuth	²¹⁴ Bi	1760	1660–1860
thorium	²⁰⁸ Tl	2615	2410–2810
total count	–	–	410–2810
cosmic	–	–	>3000

6 Energy resolution comparison

A comparative measurement under the same conditions is conducted to distinguish the energy resolution differences between the digital logarithmic airborne gamma ray spectrometer and the conventional airborne gamma ray spectrometer. The measurements make use of the natural gamma ray spectrum and the ¹³⁷Cs source spectrum for the same period using the same NaI(Tl) crystal detector and ¹³⁷Cs source at the same location. The intrinsic energy resolution of the NaI(Tl) crystal for ¹³⁷Cs is 6.6%.

Two kinds of gamma ray spectrometer were designed for testing. One has a logarithmic amplifier, as shown in Fig. 1, and the other one has similar components as show in Fig. 1 but removes the logarithmic amplifier. The linear spectrum is shown in Fig. 9(a). The logarithmic amplifier is used with the same NaI(Tl) crystal detector to measure the ¹³⁷Cs source in Fig. 9(b). Similarly, the natural gamma spectrum is measured by the linear gamma ray spectrometer shown in Fig. 9(c) and the logarithmic one is shown in Fig. 9(d).

The energy resolutions ($\Delta E(\text{FWHM})/E$) of the linear spectra and the logarithmic spectra are shown in Table 2, which indicates that the energy resolution is related to the spectrum expansion. The energy resolution improves when the channel address corresponding to the photopeak of source is expanded by the logarithmic spectrum but decreases when the channel address corresponding to the photopeak of source is condensed in the logarithmic spectrum.

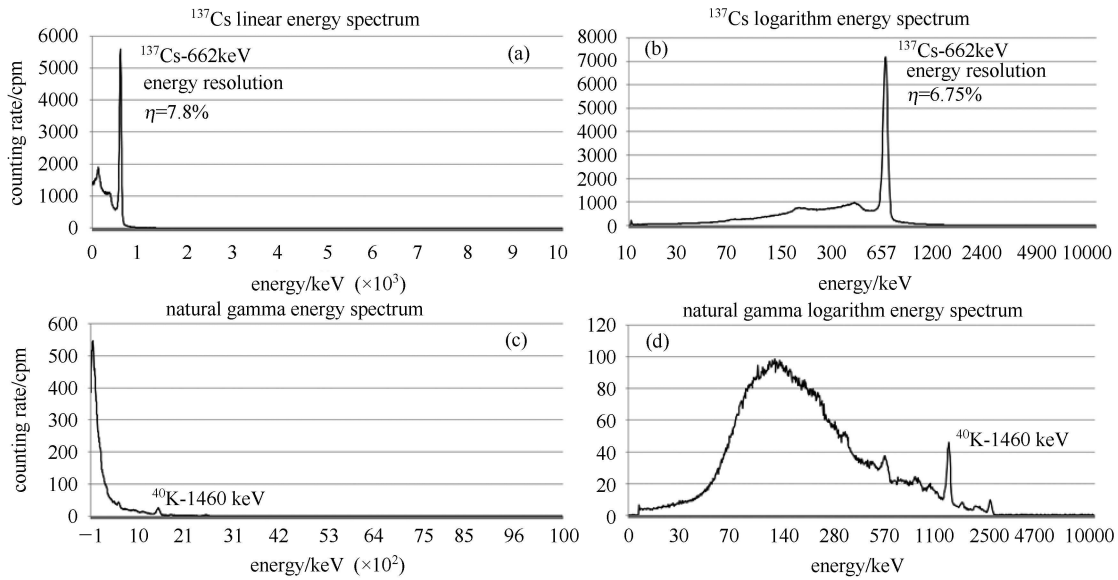


Fig. 9. Comparison between the linear spectrum and the logarithmic spectrum. (a) Linear spectrum of ^{137}Cs ; (b) Logarithmic spectrum of ^{137}Cs ; (c) Linear spectrum of natural gamma ray; (d) Logarithmic spectrum of natural gamma ray.

Table 2. Comparison between high- and low-energy resolutions.

element name	isotope used	γ -ray energy/keV	linear energy spectrum resolution	linear channel range	logarithm energy spectrum resolution	logarithm channel range
cesium	^{137}Cs	662	7.8%	71–80	6.75%	508–528
potassium	^{40}K	1460	6.12%	157–169	5.56%	616–634
thorium	^{208}Tl	2615	3.66%	264–281	4.2%	702–712

Therefore, after being logarithmically amplified (LOG114), the digital logarithmic airborne gamma ray spectrometer can increase the energy resolution of its low-energy section by 1.05% and is able to basically maintain the energy resolution of its high-energy section.

7 Conclusion

This paper describes a digital logarithmic airborne gamma ray spectrometer. This logarithmic spectrometer could maintain good resolution for both of low and high energy nuclides. Two key factors should be noted when applying this logarithmic spectrometer when the energy of the gamma rays are higher than 10 MeV: one is to choose a detector that has a higher detecting efficiency for high energy gamma rays; the other is to complete the efficiency calibration in the whole detecting energy range.

Considering these two factors, the better option is to detect a high energy gamma ray radiation source by using this logarithmic spectrometer. It should be noted that we did not consider the anti-radiation effect of this logarithmic spectrometer. Since airborne gamma ray spectrometry is an environmental radiation detecting device and its radiation dose is very low, there is no need to consider the anti-radiation effects of the electronic components. This logarithmic spectrometer cannot be used in an environment where there is a high radio activation because of the lack of overall anti-radiation evaluation. Obviously, the most effective way to improve the ability to resist radiation is to carry out lead shielding on all of the electronic units. The practical measurement proves that this system can satisfy a wide energy range measurement of a multi-crystal airborne gamma ray spectrometry survey system.

References

- 1 ZHANG Ye, XIONG Sheng-Qing, CHEN Tian-You. Applied radiation and isotopes, 1998, **49**(1-2): 139-146
- 2 ZENG Guo-Qiang, TAN Cheng-Jun, GE Liang-Quan et al. Appl. Radiat. Isot. 2014, **85**: 70-76
- 3 Sanderson D C W, Ferguson J M. Radiation Protection Dosimetry. 1997, **73**(1-4): 213-218
- 4 ZHU Meng-Hua, MA Tao, CHANG Jin. Planetary and Space Science, 2010, **58**(12): 1547-1554
- 5 Pietro Ubertini, Alessandra De Rosa, Angela Bazzano. Nucl. Instrum. Methods A, 2008, **588**: 63-71
- 6 Bizzeti P G, Carrares L, Danevich F A. Nucl. Instrum. Methods A, 2012, **696**: 144-150
- 7 Nicolas Martin-Burtart, Ludovic Guillot, Abdel-Mjid Nourredine. Applied Radiation and Isotopes. 2012, **70**: 1784-1791
- 8 Joao M R Cardoso, J Basilio Simoes, Carlos M B A. Correia. Nucl. Instrum. Methods A, 1999, **422**: 400-404
- 9 Tsankov L T, Mitev M G. Nucl. Instrum. Methods A, 2004, **533**: 509-515
- 10 Valentin T Jordanov, Glenn F Knoll. Nucl. Instrum. Methods A, 1994, **353**: 261-264
- 11 Cosimo Imperiale, Alessio Imperiale. Measurement, 2001, **30**: 49-73
- 12 Karabırdak S M, Çevik U, Kaya S. Nucl. Instrum. Methods A, 2009, **603**(3): 361-346
- 13 Analog Devices. Inc. 8/10/12/14-Bit High Bandwidth Multiplying DACs with Serial Interface: Preliminary Technical Data AD5450/AD5451/AD5452/AD5453
- 14 Karabırdak S M, Kaya S, Çevik U. Radiation Measurements, 2013, **46**: 18-23
- 15 Pece V Gorsevski, Paul E Gessler. ISPRS Journal of Photogrammetry and Remote Sensing, 2009, **64**: 184192
- 16 Michael F L'Annunziata. Handbook of Radioactivity Analysis (Third edition). USA: Academic Press Inc, 2012
- 17 Texas Instruments Inc. LOG114 Single-Supply, High-Speed, Precision Logarithmic Amplifier (Rev. A). USA: TI Inc, 2007
- 18 Acciari G. Theory and Performance of Parabolic True Logarithmic Amplifier. IEE Proceedings - Circuits, Devices and Systems, 1997
- 19 Texas Instruments Inc. REF19x Series: Precision Micropower, Low Dropout Voltage References Data Sheet. USA: TI Inc, 1996
- 20 Hovgaard J. A New Processing Technique for Airborne Gamma-ray Data. Proceedings of American Nuclear Society Sixth Topical Meeting on Emergency Preparedness and Response, 1997, 123-127
- 21 Grasty R L, John Smith B St, Minty B R S. Proceedings of Exploration 97: Fourth Decennial International Conference on Mineral Exploration. 1997, 725-732
- 22 IAEA. International Atomic Energy Agency, Technical Report Series, 1991, 323